AURORAS: The Next Evolution of Orbit Determination Using Passive Optical Observations

Jeffrey J. Bloch
Applied Research Associates, Inc.
Lynda Liptak[1,2], David Briscoe[1], Suzzanne Falvey[1], and Tasha Adams[1]
Applied Research Associates, Inc. [1]
Air Force Research Laboratory Space Vehicles Directorate (Current)[2]

ABSTRACT

In the increasingly congested space domain, accurate and timely determination of the orbital parameters of new or maneuvered objects has become critically important. Currently, any of the conventional angles-only Initial Orbit Determination (IOD) algorithms require at least three optical observations (each providing two independent angle measurements) separated significantly in time to perform well. In this paper we describe a new sensor plus algorithm engineering approach, AURORAS (Advanced Uni-sensor Rapid Orbit Reconstruction Algorithm and Sensing) (patent pending), which will dramatically improve the speed and accuracy of IOD. We obtain the minimum six independent parameters needed to define an orbit much faster than current conventional approaches by simultaneously *measuring* (not estimating) the object's angular position, angular velocity and angular acceleration at one point in time. We then proceed to describe the revolution in optical sensor technology as well as the algorithm that enables this approach. We also compare the performance of the AURORAS capability against traditional IOD methods and find that AURORAS outperforms traditional methods by an order of magnitude or more in accuracy and timeliness. We also present actual performance from one of the candidate sensors as well as a novel future sensor design (patent pending) that enables the AURORAS approach. Due to its differential nature as opposed to many traditional path integral IOD approaches, AURORAS is easily applicable to any orbital regime where the gravitational potential can be specified along the observer's line of sight at a particular point in time. This includes the Cis-Lunar environment.

1. INTRODUCTION

In the increasingly contested, congested and competitive space environment, accurate and timely Space Domain Awareness (SDA) is the key for the space arena to remain safe and usable. Determining as soon as possible the orbital parameters of new or maneuvered space objects is one of the key ingredients to enable space domain decision-making to operate within appropriately actionable timelines. Through an Independent Research and Development (IR&D) effort, Applied Research Associates, Inc. (ARA) has developed the Advanced Uni-sensor Rapid Orbit Reconstruction Algorithm and Sensing (AURORAS) approach (patent pending); a revolutionary combination of algorithmic and optical sensing capabilities that enable an unknown orbit to be estimated much faster and more accurately than current passive optical methods. The approach is applicable from Low-Earth Orbit (LEO) to cis-lunar orbits. For many important scenarios, this capability can provide critical time savings to support faster decision making. The AURORAS approach replaces the conventional measurement approach of collecting three distinct angles only observations separated in time with the *measurement* of an angle, an angular velocity, and an angular acceleration at a single point in time to determine an initial orbit.

The task of determining the unknown orbit of an object circling the Earth or Sun with separate and distinct passive optical angle measurements has had a long and strenuous scientific and technical history, as outlined in [2]. For accurate IODs from passive optical sensor observations, a general rule of thumb is that the angles data (at least three sightings) must span about an eighth of an orbit to achieve a reasonably accurate IOD. For objects near geostationary or geosynchronous orbits, this requires observations over at least three hours to determine a new object's orbit accurately. As the space domain has become more and more congested and dynamic, three hours may be too long a time to determine an object's orbit given the frequency that orbital systems can now maneuver with ever-evolving propulsion technology. In addition, the congestion of space objects (for example from a satellite or rocket body breakup, or even a large deployment of CubeSats or PLEO constellations) can make the association of

observations to each correct object difficult if the observation gaps are significant compared to the relative motion of the collection of objects. Space traffic management, debris avoidance and efficient SDA sensor tasking all now require reduced latency times between observation and accurate orbit catalog updates.

Unconventional orbits further challenge our SDA as there is exponentially increased complexity conducting orbital determination in these new orbit regimes. With so many possibilities of where a satellite may travel, SDA just became more uncertain. A faster IOD capability will decrease that uncertainty. Determining preliminary orbital information with fewer collections or in a shorter period would significantly assist the Indications and Warning (I&W) capability for characterizing evolving space events. The AURORAS algorithm and optical sensing approach enables a more accurate initial orbit to be estimated in seconds to minutes instead, which may provide critical time savings in responding to an incident in the space domain.

The key enabling development behind AURORAS is the ongoing revolutionary transformation in passive optical focal plane technology (ironically driven by other areas of the economy such as sensing for self-driving cars) that allows angle, angular velocity, and angular acceleration all to be measured independently with high precision over a short time span. We describe the algorithms and analysis (with heritage dating back to the method of Laplace) that can take these six independent angular position and motion parameters and estimate an initial orbit. We go on to describe some of the new technologies that are making this approach possible and provide a real-world example of their performance. These technologies include 1) High Time Resolution Photon Counting and Imaging Sensors, 2) Event Based (Neuromorphic) Cameras (EBCs), and 3) High Frame Rate Scientific CMOS Focal Planes (sCMOS). We present the strengths and weaknesses of each of these technologies and highlight the performance of example systems that collected data on space objects in a variety of orbits.

We also describe a notional fourth novel sensor design concept that maps angular motion into periodic photometric intensity variation measurements and the laboratory benchtop experiments that we have carried out to demonstrate the concept. These photometric measurements can then be combined with signal processing techniques to recover angular rates and accelerations.

In this paper we discuss the pros and cons of all these emerging technical approaches to obtain dynamical optical angular measurements. We model the spatial and timing resolution required to achieve this alternative IOD approach and describe the needed calibration requirements for the sensors. We show that optical sensor technology advancements on multiple fronts coupled with a re-evaluation of traditional IOD algorithms present the passive optical space surveillance community with a tipping point opportunity for disruptive innovation regarding IOD. This transformation will be as revolutionary as when optical tracking systems first changed from film to electronic focal planes.

2. THE LAPLACE METHOD REVISITED

To estimate an object's unknown orbital state, one needs to determine seven independent parameters. For a cartesian state vector representation, these parameters are position (x_n,y_n,z_n) and velocity $(\dot{x}_n,\dot{y}_n,\dot{z}_n)$ at an epoch time, t_n. For a traditional earth satellite orbital element representation (such as found in a Two Line Element (TLE) set), these parameters are: Epoch Time (t_0), Eccentricity (e), Inclination (i), Right Ascension of the Ascending Node (Ω), Mean Anomaly (M_0), Mean Motion (n), and Argument of Perigee (ω). For any orbit determination algorithm to be successful, at least six independent time stamped measurements must be obtained which will then be transformed by an algorithm into an estimate of the object's state vector or ephemeris.

The traditional approaches to the passive optical orbit determination involve three angles-only measurements taken by an observer separated in time by some fraction of the object's orbital period. Each angular observation results in two time-stamped numbers; azimuth and elevation $((t_1,az_1,el_1),(t_2,az_2,el_2),(t_3,az_3,el_3))$ or right ascension and declination $((t_1,\alpha_1,\delta_1),(t_2,\alpha_2,\delta_2),(t_3,\alpha_3,\delta_3))$. Hence, three observations result in six independent angle measurements. The various IOD methods then take these measurements and either through a direct or iterative solution method estimate an orbital state vector, usually for the second or middle time of the three observations. These methods fall into two broad categories.

Methods in the first category estimate the object's angular velocity and angular acceleration at the second time (t_2) observation by an interpolation procedure using all three measurements and then by direct inversion or iteration solves for range and range rate for the second observation. Two issues constrain this type of approach. If the observations are too far apart, the interpolation methods to deduce the angular motion derivatives at the second observation time become inaccurate due to the changing nature of the object's angular acceleration and the changing angular acceleration and velocity of the observer. If the observations are too close together, the uncertainties in the observations themselves (timing and angular measurement) contribute to large uncertainties in the angular derivatives due to the short time baselines.

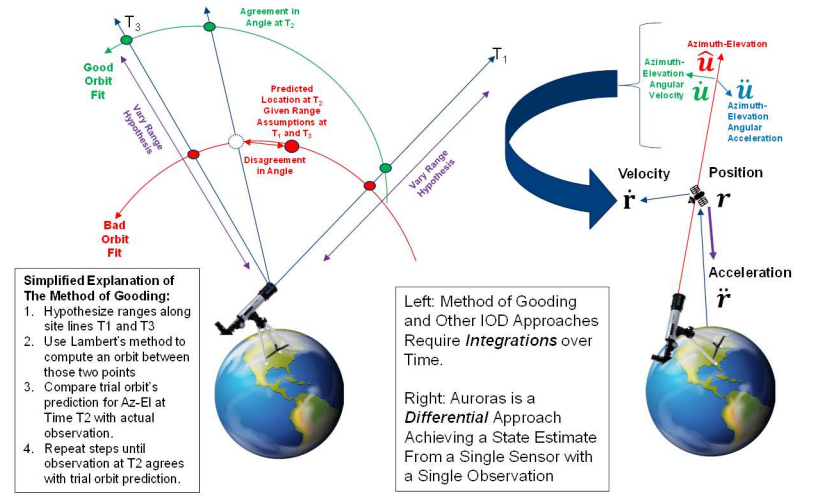

Figure 1 – Comparison of a current standard IOD procedure (left) with AURORAS (right).

The second category involves direct geometric analysis of all three observations. Some members of this category (such as the method of Gooding [8]) iterate ranges for the first and third observations trying to match the second observation using lambert's theorem to predict the object's location at the middle observation time. Other types (such as Gauss's method [6]) try a direct solution of the orbit using geometrical properties (such as that the orbital motion lies in a plane) and the algebraic inversions of series representations of the f and g functions (which describe how the motion evolves from an initial position and velocity at a given time). Such approaches get more accurate when the time interval between observations increases, therefore when only short timelines are available, the accuracy will be low. Comparing this type of IOD to AURORAS is shown in Figure 1.

The key idea behind the AURORAS approach is that new optical sensor technology allows the relatively direct and simultaneous measurement of angles, angular velocities, and angular accelerations. (This approach was first explored briefly in reference[15]). With this in mind, we will now revisit Laplace's IOD approach. For the following derivation the variable definitions are defined in the left box below. The vectors describing the observations of angle, angular velocity and angular acceleration on the unit sphere have the vector multiplication properties as showen in the right box.

$\boldsymbol{r}$ = Target Position at time t with respect to Earth Center
$\hat{\boldsymbol{u}}$ = Observation Vector from Observer of Target at time t
$\dot{\boldsymbol{u}}$ = Angular Velocity Vector of Target as Seen By Observer at Time t
$\ddot{\boldsymbol{u}}$ = AngularAcceleration Vector of Target as Seen By Observer at Time t
$\boldsymbol{r}_{observer}$ = Positon of Observer at Time t
$\dot{\boldsymbol{r}}_{observer}$ = Velocity of Observer at Time t
$\ddot{\boldsymbol{r}}_{observer}$ = Acceleration of Observer at Time t
ρ = Range to Satellite from Observer at Time t
$\dot{\rho}$ = Range Rate to Satellite from Observer at Time t
$\ddot{\rho}$ = Range Acceleration of Satellite from Observer at Time t
$GM_{\oplus}$ = Gravitaional Constant
$\boldsymbol{r}, \dot{\boldsymbol{r}}$ ≡ **Target State Vector at Time t**
$\ddot{\boldsymbol{r}}$ ≡ **Target Acceleration Vector at Time t**

$$\hat{\boldsymbol{u}} \cdot \hat{\boldsymbol{u}} = 1$$
$$\hat{\boldsymbol{u}} \cdot \dot{\boldsymbol{u}} = 0$$
$$\hat{\boldsymbol{u}} \cdot \ddot{\boldsymbol{u}} = -|\dot{\boldsymbol{u}}|^2$$
$$(\hat{\boldsymbol{u}} \times \dot{\boldsymbol{u}}) \cdot \hat{\boldsymbol{u}} = \boldsymbol{0}$$
$$(\hat{\boldsymbol{u}} \times \dot{\boldsymbol{u}}) \cdot \dot{\boldsymbol{u}} = \boldsymbol{0}$$
$$(\hat{\boldsymbol{u}} \times \ddot{\boldsymbol{u}}) \cdot \hat{\boldsymbol{u}} = \boldsymbol{0}$$
$$(\hat{\boldsymbol{u}} \times \ddot{\boldsymbol{u}}) \cdot \ddot{\boldsymbol{u}} = \boldsymbol{0}$$

At a fixed time, the position of a space object in orbit can be expressed in terms of the observer's position:

$$\boldsymbol{r} = \rho\hat{\boldsymbol{u}} + \boldsymbol{r}_{observer} \quad (1)$$

The derivatives of the object's motion are straightforward to express:

$$\dot{\boldsymbol{r}} = \dot{\rho}\,\hat{\boldsymbol{u}} + \rho\dot{\boldsymbol{u}} + \dot{\boldsymbol{r}}_{observer} \quad (2)$$

$$\ddot{\boldsymbol{r}} = \ddot{\rho}\hat{\boldsymbol{u}} + 2\dot{\rho}\dot{\boldsymbol{u}} + \rho\ddot{\boldsymbol{u}} + \ddot{\boldsymbol{r}}_{observer} \quad (3)$$

While the spatial position and spatial velocity of the object are arbitrary, the acceleration of the object (assuming no perturbing forces or thrusting) is defined by gravity:

$$\ddot{\boldsymbol{r}} = \frac{-GM_{\oplus}\boldsymbol{r}}{|\rho\hat{\boldsymbol{u}}+\boldsymbol{r}_{observer}|^3} \quad (4)$$

While we use the simple two body formula for acceleration here, any more complex gravitational field model can be substituted, thus enabling use in the Cis-Lunar environment, as well as models of earth's gravity involving spherical harmonic terms. Equating the expressions for the object's acceleration from observation and gravity yields:

$$\ddot{\rho}\hat{\boldsymbol{u}} + 2\dot{\rho}\dot{\boldsymbol{u}} + \rho\ddot{\boldsymbol{u}} = \frac{-GM_{\oplus}\boldsymbol{r}}{|\rho\hat{\boldsymbol{u}}+\boldsymbol{r}_{observer}|^3} - \ddot{\boldsymbol{r}}_{observer} \quad (5)$$

In order to simplify the equation and reduce the number of variables to solve for we employ a vector multiplication trick:

$$(\hat{\boldsymbol{u}} \times \dot{\boldsymbol{u}}) \cdot (\ddot{\rho}\hat{\boldsymbol{u}} + 2\dot{\rho}\dot{\boldsymbol{u}} + \rho\ddot{\boldsymbol{u}}) = (\hat{\boldsymbol{u}} \times \dot{\boldsymbol{u}}) \cdot \left(\frac{-GM_{\oplus}(\rho\hat{\boldsymbol{u}} + \boldsymbol{r}_{observer})}{|\rho\hat{\boldsymbol{u}} + \boldsymbol{r}_{observer}|^3} - \ddot{\boldsymbol{r}}_{observer}\right) \quad (6)$$

$$\rho(\hat{\boldsymbol{u}} \times \dot{\boldsymbol{u}}) \cdot \ddot{\boldsymbol{u}} - (\hat{\boldsymbol{u}} \times \dot{\boldsymbol{u}}) \cdot \left(\frac{-GM_{\oplus}(\rho\hat{\boldsymbol{u}}+\boldsymbol{r}_{observer})}{|\rho\hat{\boldsymbol{u}}+\boldsymbol{r}_{observer}|^3} - \ddot{\boldsymbol{r}}_{observer}\right) = 0 \quad (7)$$

Equation (7) can now be solved numerically for the range to object from the observer (ρ) given that the angle, angular velocity, and angular acceleration of the object at time t has been provided by sensor data. The simple interpretation of equation (7) is that the range to the object must be such that projection on the sky of the gravitational acceleration of the object has to match the apparent angular acceleration. Once we have solved for ρ, we can solve for the range-rate ($\dot{\rho}$) term thusly:

$$\dot{\boldsymbol{u}} \cdot (\ddot{\rho}\hat{\boldsymbol{u}} + 2\dot{\rho}\dot{\boldsymbol{u}} + \rho\ddot{\boldsymbol{u}}) = \dot{\boldsymbol{u}} \cdot \left(\frac{-GM_{\oplus}(\rho\hat{\boldsymbol{u}}+\boldsymbol{r}_{observer})}{|\rho\hat{\boldsymbol{u}}+\boldsymbol{r}_{observer}|^3} - \ddot{\boldsymbol{r}}_{observer}\right) \quad (8)$$

$$2\dot{\rho}|\dot{\boldsymbol{u}}|^2 + \rho(\dot{\boldsymbol{u}} \cdot \ddot{\boldsymbol{u}}) = \dot{\boldsymbol{u}} \cdot \left(\frac{-GM_{\oplus}\boldsymbol{r}}{|\rho\hat{\boldsymbol{u}}+\boldsymbol{r}_{observer}|^3} - \ddot{\boldsymbol{r}}_{observer}\right) \quad (9)$$

$$\dot{\rho} = \left[\frac{\dot{\boldsymbol{u}} \cdot \left(\frac{-GM_{\oplus}(\rho\hat{\boldsymbol{u}}+\boldsymbol{r}_{observer})}{|\rho\hat{\boldsymbol{u}}+\boldsymbol{r}_{observer}|^3} - \ddot{\boldsymbol{r}}_{observer}\right) - \rho(\dot{\boldsymbol{u}} \cdot \ddot{\boldsymbol{u}})}{2|\dot{\boldsymbol{u}}|^2}\right] \quad (10)$$

Once ρ and $\dot{\rho}$ are solved for, the state vector $(\boldsymbol{r}, \dot{\boldsymbol{r}})$ at time t can be obtained using equations (1) and (2).

The sensors described in this paper produce dynamic measurements in terms of angles on the sky and not vectors on the unit sphere. To compute the observational direction vector measurement and associated derivatives ($\hat{u}, \dot{u}, \ddot{u}$)from dynamical spherical angular measurements ($\alpha,\delta,\dot{\alpha},\dot{\delta}, \ddot{\alpha},\ddot{\delta}$) at time t, we need the following vector formulas:

$$\hat{u} = \begin{bmatrix} \cos\delta\cos\alpha \\ \cos\delta\sin\alpha \\ \sin\delta \end{bmatrix} \quad (11)$$

$$\dot{u} = \begin{bmatrix} -\dot{\delta}\sin\delta\cos\alpha - \dot{\alpha}\cos\delta\sin\alpha \\ -\dot{\delta}\sin\delta\sin\alpha - \dot{\alpha}\cos\delta\cos\alpha \\ \dot{\delta}\cos\delta \end{bmatrix} \quad (12)$$

$$\ddot{u} = \begin{bmatrix} -\ddot{\delta}\sin\delta\cos\alpha - \dot{\delta}^2\cos\delta\cos\alpha + 2\dot{\alpha}\dot{\delta}\sin\delta\sin\alpha - \dot{\alpha}^2\cos\delta\cos\alpha - \ddot{\alpha}\cos\delta\sin\alpha \\ -\ddot{\delta}\sin\delta\sin\alpha - \dot{\delta}^2\cos\delta\sin\alpha - 2\dot{\alpha}\dot{\delta}\sin\delta\cos\alpha - \dot{\alpha}^2\cos\delta\sin\alpha + \ddot{\alpha}\cos\delta\cos\alpha \\ \ddot{\delta}\cos\delta - \dot{\delta}^2\sin\alpha \end{bmatrix} \quad (13)$$

With these formulations, we are now ready to exploit the new optical sensor capabilities to obtain an IOD.

3. THE OPTICAL SENSOR REVOLUTION THAT ENABLES AURORAS

From the time of Hipparchus using an astrolabe over 2000 years ago to today's advanced optical angular measurement sensors such as the Space Surveillance Telescope, optical position measurements of objects in the night sky have always been a series of fixed angles at fixed times. Modern passive optical systems collect an

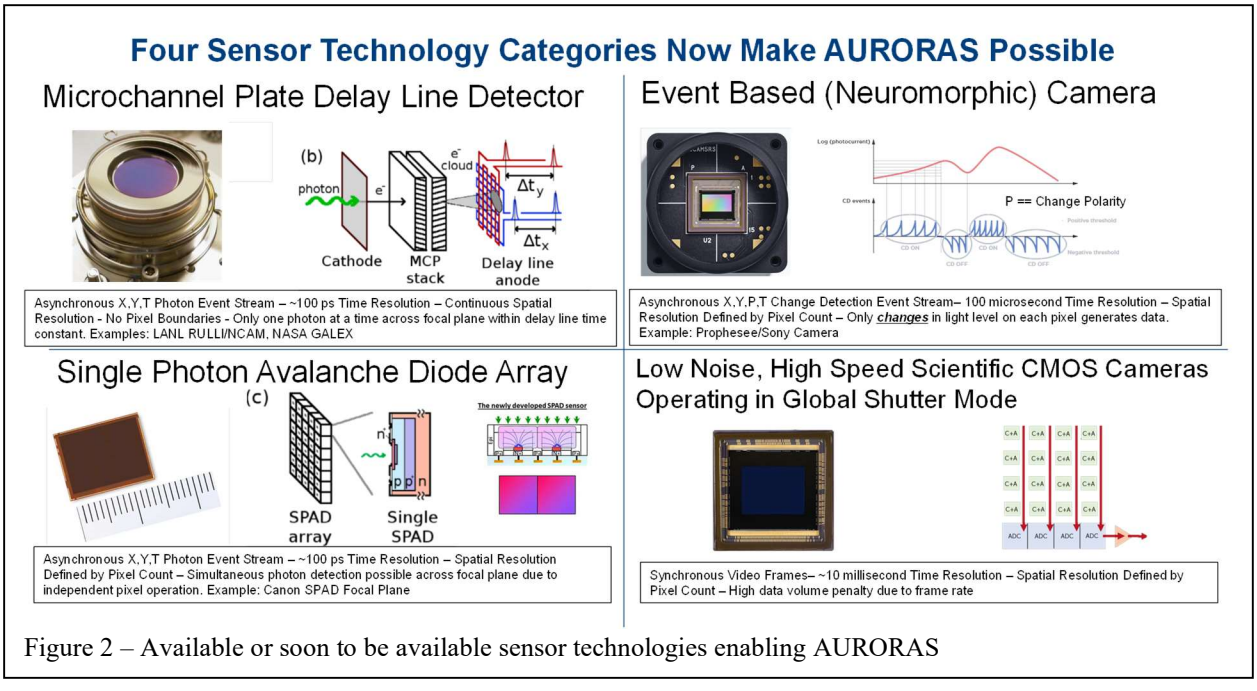

Figure 2 – Available or soon to be available sensor technologies enabling AURORAS

electronic image of sky in which image pixel locations map onto celestial angular coordinates. Moving objects against the stellar background in the image produce multi-pixel "streaks" or "tracks" whose end points represent the angular position of the object at the beginning and end of the image exposure. These end-point coordinates from multiple images are then fed to an orbit determination algorithm along with information about the observer's location. Unfortunately, due to past technological limitations, the signal in the "streak" between endpoints can not be used for orbit determination because all the moving object's dynamical information is lost in the photon collection

process that created the image. Shorter image exposures to recover high time resolution data were previously limited in applicability by the penalty of high readout noise per image frame. Also, achieving high time resolution measurements for optical image collection required careful system design of the optical shutter system. Mechanical shutters or rolling electronic shutters introduce pixel location dependent exposure timing effects. For framing sensors, true global electronic shutters are essential.

The original breakthrough enabling electronic imaging for astronomical applications came with the advent of Charge Coupled Device (CCD) imagers with significant pixel format sizes[11]. A CCD chip consists of a pixel array of p-doped metal–oxide–semiconductor (MOS) capacitors that collect photo-electrons from an epitaxial photoactive region during an image exposure. The capacitors can be thought of as an array of "buckets" collecting photon "raindrops" in the form of photo-electrons. When the image exposure is complete, the buckets of photo-electron charge are transferred from pixel capacitor to pixel capacitor like a bucket brigade first down pixel columns and then down a pixel row to a charge readout amplifier and digitizer to obtain a photon flux signal value collected in each pixel. Faster readouts and charge transfers increased the read noise in the reported signal values thus limiting fast frame rates for low light applications requiring high time resolution with short frame to frame exposures.

However, over the last 20 years or so, several optical imaging sensor technologies have dramatically evolved to achieve better time resolution, larger spatial format, better detection sensitivity and lower readout and background noise over the original Charge Coupled Device (CCD) chips. These include Electron Multiplied Charge Coupled Devices (EMCCDs)[19], Scientific Complementary Metal-Oxid Semiconductors (sCMOS)[19][20][21], microchannel plate (MCP) based photon counting imaging sensors[12][13][14][15][16], Neuromorphic Event Based Cameras (EBCs)[17], and the exciting emerging technology of large format Single Photon Avalanche Diode (SPAD) arrays[21][22][25]. These technologies are overviewed in Figure 2.

These new sensor advancements allow the time and spatial (angular) measurement of the the arrival of photons or groups of photons on the sensor focal plane with resolution not previously possible and now enable the AURORAS approach to IOD. However, for the very high time and good spatial resolution required for AURORAS, we will put aside EMCCDs as a candidate due to lagging capabilities compared with the other technologies. Table 1 presents a brief overview of the strengths and weakness of these technologies as applied to AURORAS.

Technology	Time Resolution	Dark Background Events/Electrons Rate Per Resolution Element or Pixel	Spatial Calibration Issues	Data Volume/Processing Issues	Cost
MCP/Delay Line	100 picoseconds	0.005 Events/Second (Almost Every Event Is a Signal Photon)	Pixel-less Sensor; Non-linearities in delay line timing cause subtle spatial distortions that must be calibrated out.	Photon Event Stream Provides Natural Data Compression.	$$$
SPAD Array	100 picoseconds	1-10 Events/Second	None	Photon Event Stream Provides Natural Data Compression.	$?
Event Based Camera	~100 microseconds	~1-10 Events/Second	Astrometric Calibration requires stars to move, i.e. sidereal tracking will provide no reference stars.	Change Detection Event Stream Provides Natural Data Compression	$
High Speed/Low Noise Scientific CMOS	1.5 milliseconds (660 f/s)	~2000 Electrons/ Second	None	Huge Data Volume, Needs Significant Real Time Analysis and Object Extraction	$$

Exceeds Requirements | Meets Requirements | Problematic But Issue Can Be Mitigated | May Be a Serious Hinderance

Table 1 – Comparison of the performance parameters of AURORAS candidate sensors

4. BENCHMARK SIMULATIONS

4.1. Simulation Overview

Dolado, Yanez and Alfredo[10] published a comprehensive benchmark of current IOD methods using passive optical measurements of varying accuracy against a variety of objects in different orbits, including LEO, MEO, GTO and GEO regimes. The paper described the orbits, observer position and observation times used for the

benchmarks. In Table 1 of that paper [10], the authors summarize the strengths and weaknesses of eight IOD methods, and then proceed to select five methods for their benchmark study. These methods included Gauss[6], Gauss Iterative[2], Gooding[8], Baker-Jacobi[7] and Karimi – Mortari (Jn and Ln methods)[9]. The observer for the benchmark simulations was placed at the ground-station location of the TAROT telescope at Calern, France (6.9238E, 43.7522N, 1270.0 m). Optical observations were simulated with no measurement error, 0.3 mdeg measurement error and 3 mdeg measurement error. (mdeg = milli-degree = 0.001 degree = 3.6 arcseconds) Figure 3 contains the outline for the orbits for simulated objects in the study.

To compare this paper's benchmarks with AURORAS, we postulated the use of a photon counting imaging detector where each photon could be measured with no error, 0.3 mdeg error variance and 3 mdeg error variance. We further postulated a detected photon rate of 1000 events/second. For a telescope with a 30cm aperture, a V band filter and an overall system efficiency of 50%, this corresponds to an object with an optical magnitude between 13 and 14 which covers many space optical surveillance scenarios. More specifically, if we postulate a 36 cm aperture Rowe-Ackerman Schmidt Astrograph[24] with a SPAD sensor[25], we estimate similar performance. We also assume high resolution timing for each photon, at the microsecond or better level. As reported in the previous section, such performance is now within reach through multiple focal plane technology approaches.

Dolado, Yanez and Alfredo[10] simulate three optical observations of the benchmark objects separated by different times as outlined in Appendix B of that paper. To do the comparison, the simulated AURORAS sensor operated continuously over twice the period listed in each case in the Appendix B table, corresponding to a continuous collection of photon events from the time of the paper's first optical observation to the third (last) observation as shown in the upper left of Figure 3.

4.2. Analysis of and Comparison Simulated Data with Published Benchmarks

The upper left of figure 3 shows how AURORAS observations were simulated compared to the benchmark paper optical observations. Figure 4 shows a representative analysis of an AURORAS observation of a benchmark orbit.

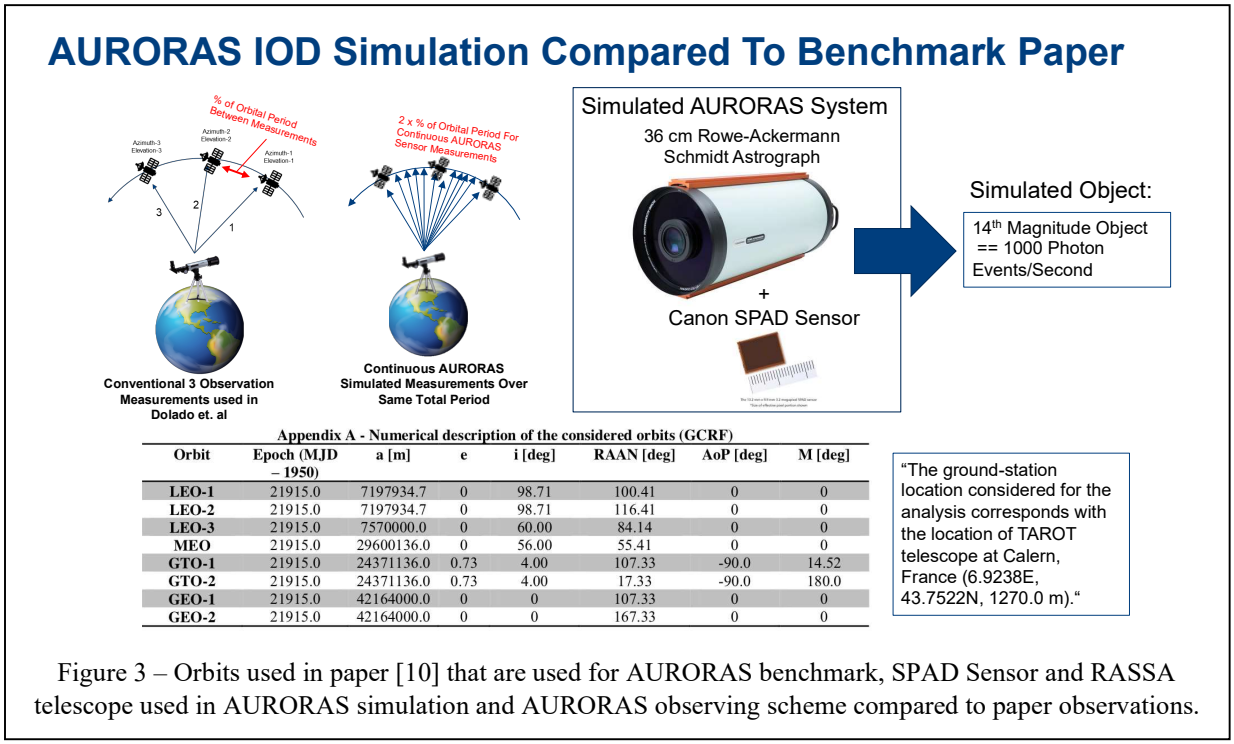

Figure 3 – Orbits used in paper [10] that are used for AURORAS benchmark, SPAD Sensor and RASSA telescope used in AURORAS simulation and AURORAS observing scheme compared to paper observations.

Figures 5a and 5b show the results of the analysis of simulated AURORAS data against the paper benchmark results. The AURORAS approach with a SPAD Sensor (EBC sensor will produce very similar results) mounted on a notional RASSA telescope outperforms in accuracy and timeliness conventional optical angle observations with conventional IOD algorithms by over an order of magnitude in most cases.

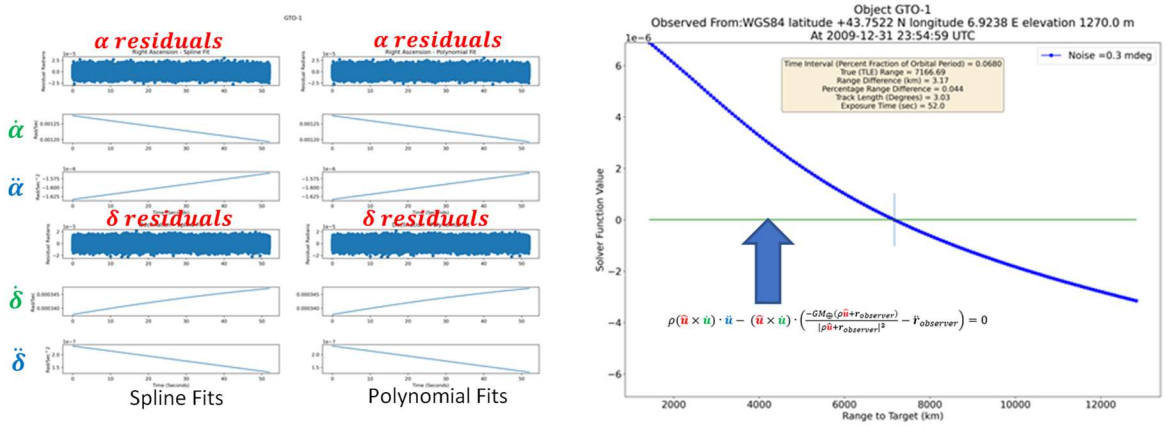

Figure 4 – Example analysis of simulated AURORAS benchmark comparison data.

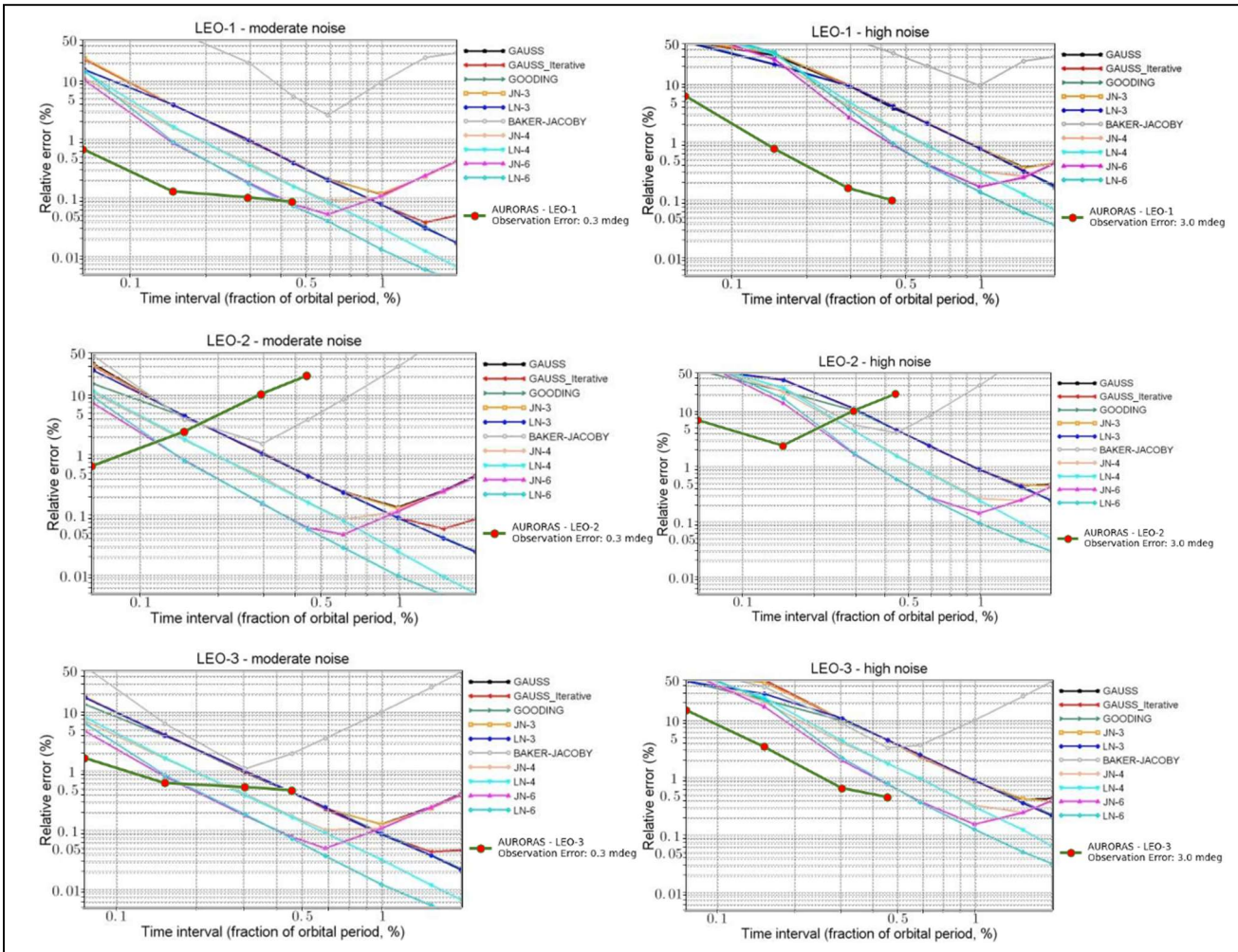

Figure 5a -AURORAS IOD performance with a simulated RASSA telescope and SPAD sensor compared to the benchmark paper results with conventional optical observations and IOD algorithms. The "Time interval" represents the time between the first and second, and then second and third observation for the original paper benchmark

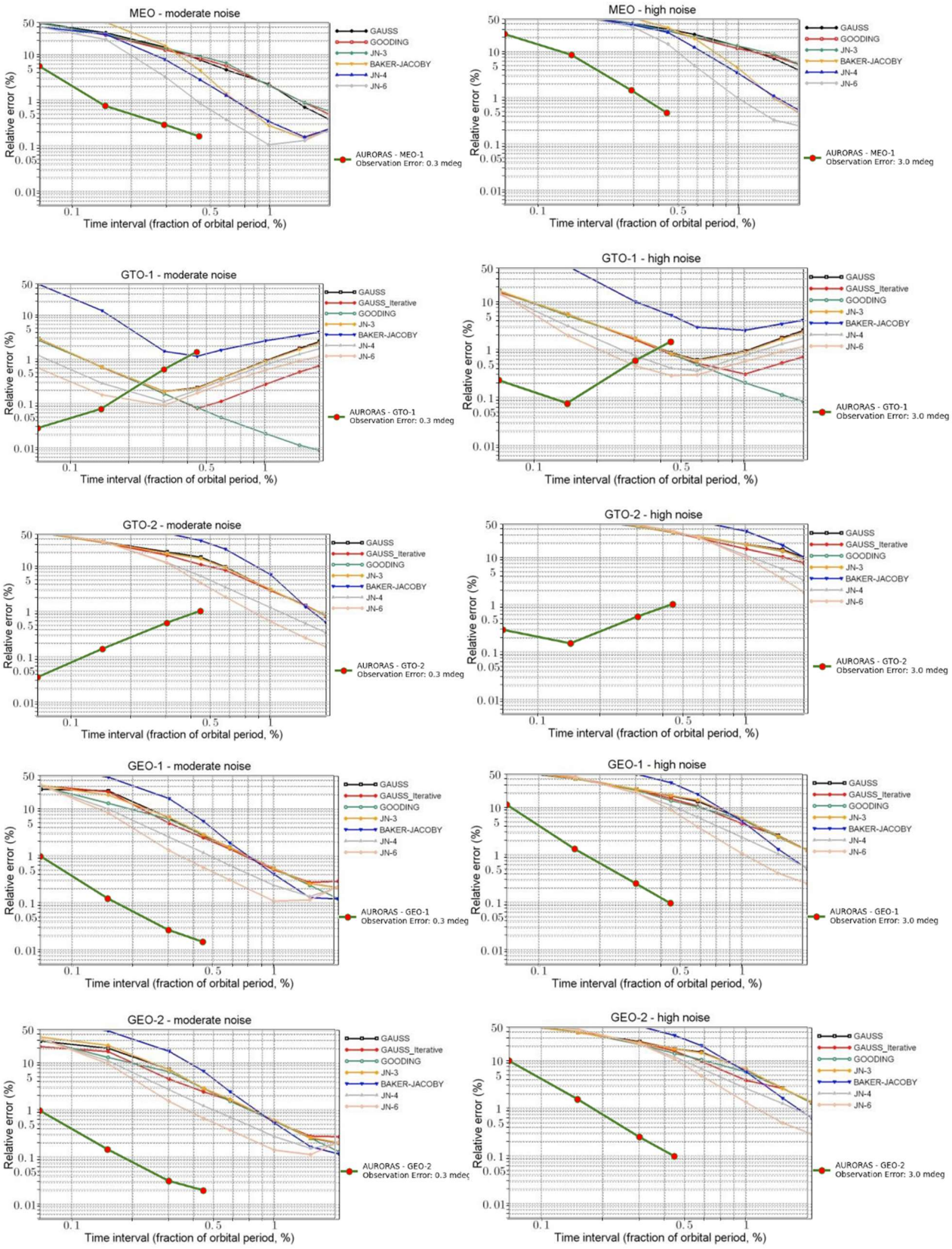

Figure 5b -Continued - AURORAS IOD performance with a simulated RASSA telescope and SPAD sensor compared to the benchmark paper results with conventional optical observations and IOD algorithms.

5. EXAMPLE APPLICATION – THE EVENT BASED CAMERA

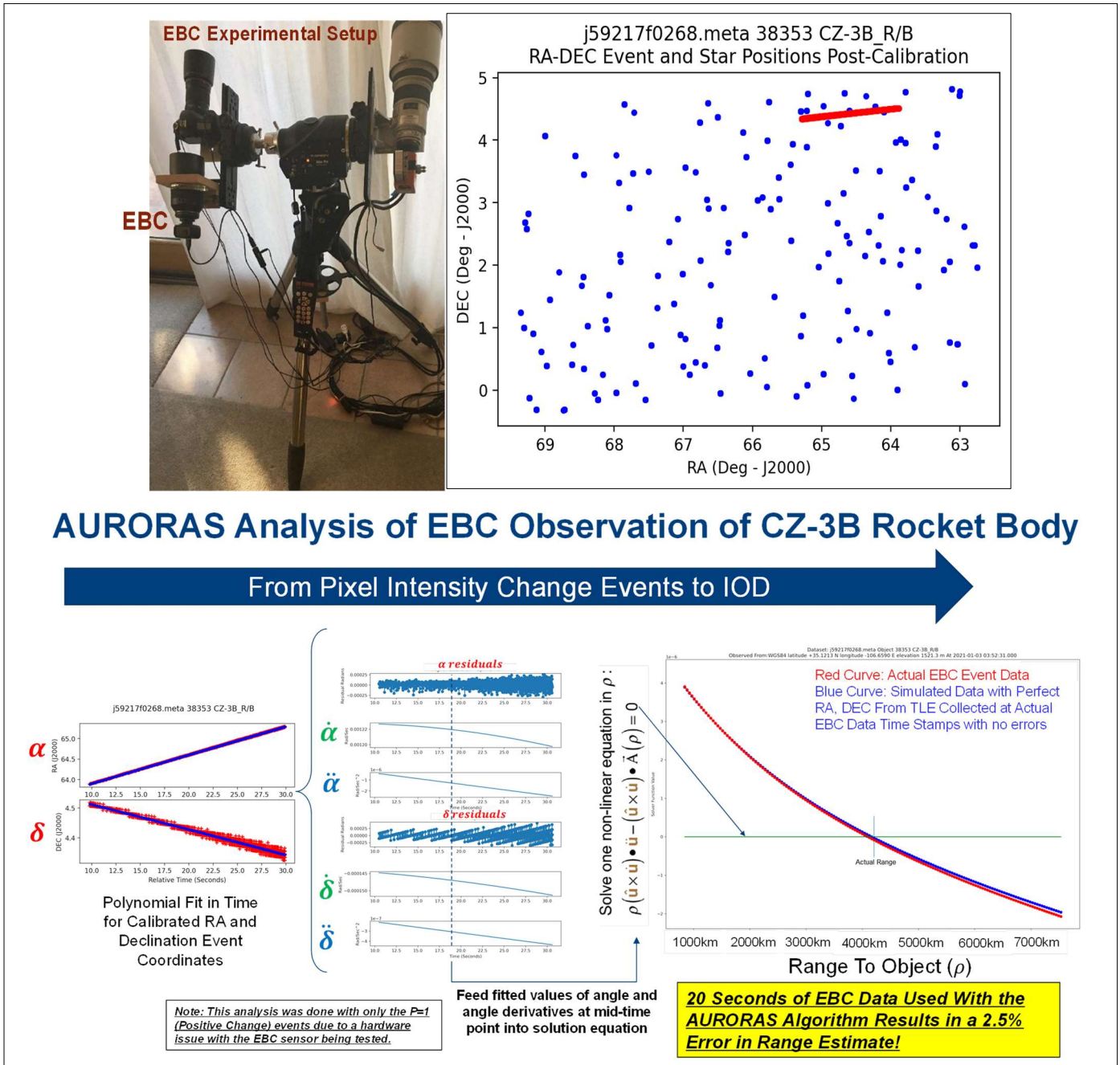

Figure 6. AURORAS technique applied to EBC data on Chinese rocket body CZ-3B. Top: EBC experimental setup and Post calibration event data for the object and star positions. Bottom: Object event data RA and DEC fit vs. time, recovering angular velocities and accelerations leading to a solution to the nonlinear equation deriving the range to target with 3% accuracy.

The authors teamed with AFRL/RV scientist, Dr. Dave Monet, who had collected EBC data using the setup shown in the top right of figure X and obtained 762 EBC space object collections. We analyzed the set using the AURORAS approach using the angles, angular velocity, and angular acceleration and estimated the range and range rate for various space objects. Many of the EBC datasets produced good range determination results. However, the

optical setup was not optimized for this use, and the data was collected before the concept to test this differential approach of initial orbit determination was developed. Thus, a large portion of the data was not ideal for this exercise and did not yield good results. Yet, a significant amount of data was "cooperative" for this approach – the first validation of the concept with an Event Based Camera.

Comparison of the analysis of simulated (pixelated) EBC event data with the same time stamps as the actual data (and backward RA-DEC to focal plane Row-Column calibration) indicates that the angular pixel size was responsible for most of the failures to solve for the correct range and range rate. For all these datasets, if the algorithm is applied to "perfect data" (right ascension and declination from a catalog that is computed from the object's ephemeris at each event time stamp) the true range and range rate are always successfully obtained. Future AURORAS tests with this EBC focal plane would need to have a re-designed optical system with a smaller field of view.

As an example of the successful results (Figure 6), we calculated the range determination comparison for a Chinese CZ-3B rocket body by applying the AURORAS algorithm to truth (from Space-Track.org ephemeris), simulated data and actual EBC data. The EBC measurements produced a range estimate within 3% of the Space-Track.org prediction, a very accurate result using ground-based observations over a very short time period with non-optimized COTS equipment.

6. ADVANCED SENSOR CONCEPT: AFRAME

In the past the lead author (Bloch) has had numerous conversations with members of the astrodynamics community on whether high density passive optical observations bring anything new to the IOD problem in terms of "information observability". As a "gedankenexperiment" and as a novel alternative approach to measure angle,

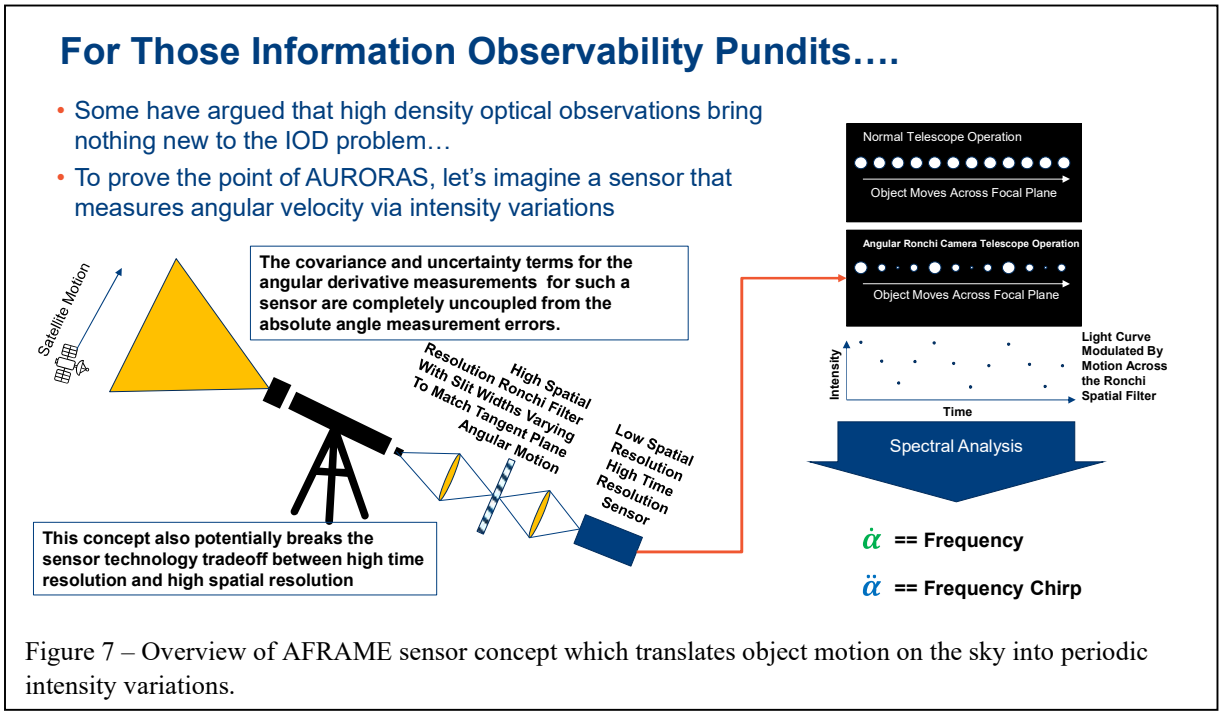

Figure 7 – Overview of AFRAME sensor concept which translates object motion on the sky into periodic intensity variations.

angular velocity and angular acceleration simultaneously and directly we present a novel sensor concept to amplify the concept behind the AURORAS approach. This concept, called AURORAS Frequency Representation of Angular Motion Experiment or AFRAME (patent pending), translates object motion in the field of view to periodic light intensity variations whose frequency and frequency change (chirp) represents a direct measurement of angular motion quantities. Such a setup explicitly uncouples the error covariance terms of absolute angular position from angular motion quantities. Figure 7 depicts the high-level overview of the concept using a low spatial resolution,

high time resolution camera coupled with a high spatial resolution Ronchi filter. Such a concept approaches the distinct covariance properties that the radar community has enjoyed with separately measuring radar pulse round trip times vs. pulse doppler shift to separately measure range and range rate.

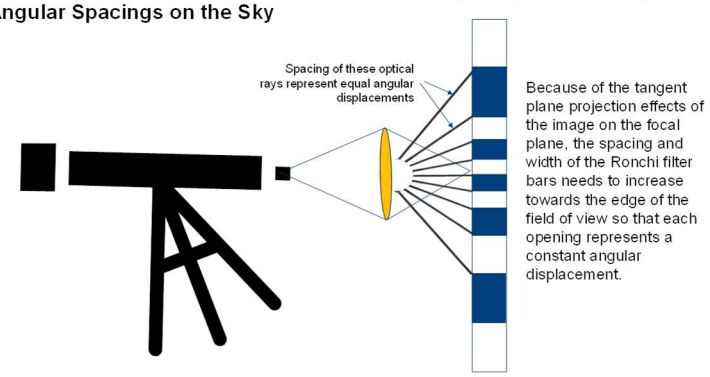

Figure 8 – The openings of the Ronchi slits must be variable so each opening represents a constant change in angular displacement on the sky.

Several detailed design features are needed to make the AFRAME concept work. First, a single temporal frequency in brightness variation should represent a fixed angular velocity across the sensor field of view. Because a sensor's focal plane surface represents a tangent plane projection of the sky, fixed angular increments going across the field of view represent larger and larger incremental spatial distances on the focal plane going from the center to the edge. (See Figure 8) As a result, we must postulate a Ronchi spatial filter with varying open spacings so that each opening represents a constant angular displacement.

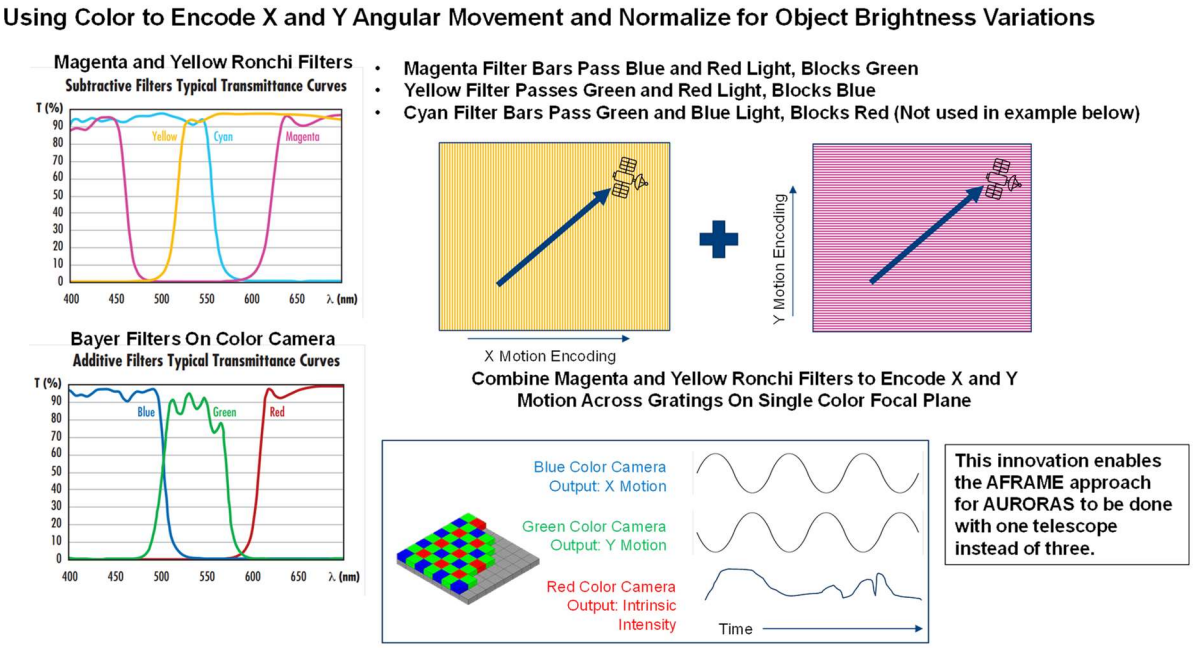

Figure 9 – Enabling the AFRAME concept with one telescope and focal plane using subtractive color filters in orthogonal Ronchi filter bars and a color focal plane with Bayer color transmittance filters on its pixels.

Another AFRAME design feature must allow for the angular position and motion of an object to be measured in two orthogonal directions. In addition, the AFRAME concept must consider the fact that many space objects intrinsic light curves are variable and can be periodic due to object spin or rotation. Both needs could be met using three co-aligned telescopes. Two telescopes would each have a variable spacing Ronchi filters oriented orthogonal to the

other Ronchi equipped telescope, and the third telescope would have no Ronchi filter and would be used to measure the intrinsic brightness variations of the object to normalize the readings from the other two telescopes.

However, there is a way to accomplish these requirements using one telescope as outlined in Figure 9. Consider using a high-speed low spatial resolution color focal plane (pixels with red, green, blue bayer filters) and replacing the solid bars of a Ronchi filter with subtractive color filter material. If two orthogonal Ronchi filters using magenta and yellow color bars are placed at the intermediate focus, the blue and green images from the color camera will encode motion in the two orthogonal directions, while the red images would track the overall brightness variations of the object and would be used to normalize the measurements for the blue and green images.

With the AFRAME sensor concept in mind, it is easy to see to first order that the covariance errors in measuring the frequency of light variations measuring angular motion would be explicitly de-coupled from the fixed pointing error covariance of the telescope. The outputs from an AFRAME system would provide independent measurements (in covariance sense) of angle, angular rate, and angular acceleration for the AURORAS algorithmic approach.

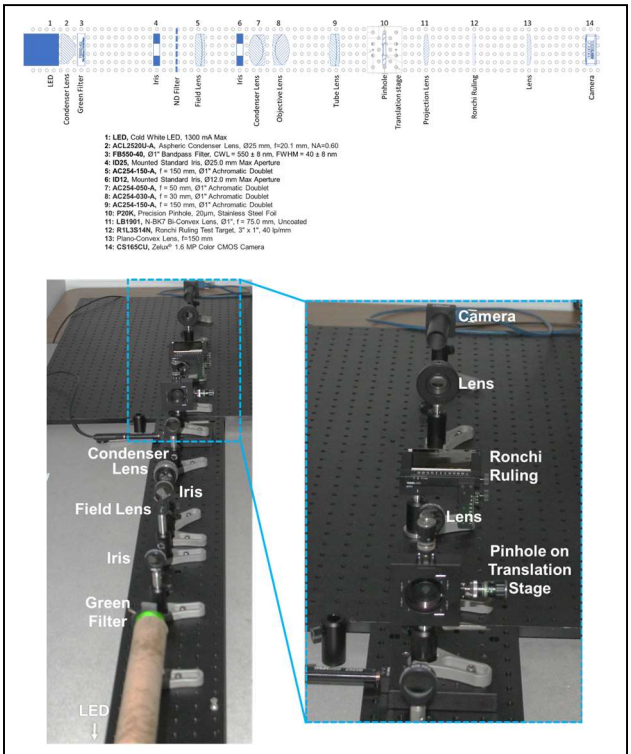

Figure 10 – Top: Optical layout for AFRAME bench test. Bottom: Photos of the experimental setup.

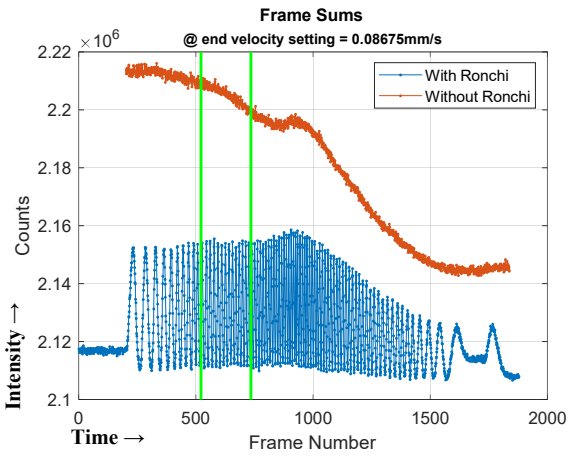

Figure 11 – Preliminary experimental results from AFRAME benchtop experiment showing how the frequency of the intensity changes of the object spot increases and then decreases at the motor stage moving the source accelerates and then decelerates between positions. This plot also shows the need to independently measure the intrinsic intensity changes in the brightness of the object image spot so that the periodic intensity signal can be normalized.

We have taken the first steps to demonstrate AFRAME sensor concept in the laboratory. Figure 10 shows the experimental benchtop setup. Figure 11 shows some of the raw laboratory data demonstrating the periodic intensity variations changing with angular velocity and acceleration.

7. CONCLUSIONS

The AURORAS (patent pending) approach has revealed that passive optical space surveillance for orbit determination is on the brink of a revolution as important prior transitions when photographic film-based systems transitioned to EBSicon/Vidicon electronic sensors and then to framing CCD and then CMOS focal planes. Each of these transitions marked a significant improvement in spatial resolution and timing performance. Event Based (Neuromorphic) Cameras (EBC), Imaging Photon Counters (IPC), Single Photon Avalanche Photodiode (SPAD)

Arrays and Scientific CMOS (sCMOS) focal planes have all pushed optical spatial and timing measurement capabilities to where the dynamical motions of objects in orbit can be measured with timing and angular resolution and format never before possible. We have shown that such measurement capabilities allow Initial Orbit Determination (IOD) to be performed with an order of magnitude more accuracy and precision on timescales much shorter than previously possible. Other concepts, such as AFRAME will likely amplify these capabilities in the future.

In this paper we have focused on the IOD problem specifically. Once an accurate IOD is obtained, the same high density optical observations can be passed to Sequential Batch or Kalman filter algorithm to further refine the result. These techniques require accurate initial guesses to be effective. Future work will explore this synergy.

8. REFERENCES

[1] Escobal, P.R.: Methods of orbit determination. Wiley, New York (1965). Sect. 7.4

[2] Vallado, D.A. Fundamentals of astrodynamics and applications, 3rd edn. Microcosm Press, Hawthorne (2007). Sect. 7.3.1

[3] Roy, A.E. Orbital motion, 4th edn. Taylor & Francis, New York (2005). Sect. 14.3

[4] Bate, R.R., Mueller, D.D., White, J.E.: Fundamentals of astrodynamics. Dover, New York (1971). Sect. 2.11

[5] Prussing, J.E., Conway, B.A. Orbital mechanics, 2nd edn. Oxford University Press, Oxford (2013). Sect. 14.3

[6] Gauss, C. F. Theoria motus corporum coelestium in sectionibus conicis solem ambientium Hamburg: Friedrich Perthes and I.H. Besser, 1809.

[7] R. M. L. Baker and N. H. Jacoby , Preliminary orbit-determination method having no co-planar singularity. Celestial Mechanics (1977) 15 : 137-160

[8] R. H. Gooding. A new procedure for the solution of the classical problem of minimal orbit determination from three lines of sight. Celestial Mechanics Dynamical Astronomy (1997) 66 : 387-423

[9] R.R. Karimi and D. Mortari. Initial orbit determination using multiple observations. Celest Mech Dyn Astr (2011) 109:167-180

[10] Dolado, Juan & Yanez, Carlos & Anton, Alfredo. (2016). On the performance analysis of Initial Orbit Determination algorithms. 67th International Astronautical Congress (IAC), Guadalajara, Mexico, 26-30 September 2016.

[11] Janesick, James R., Society of Photo-optical Instrumentation Engineers, and SPIE Digital Library. Scientific Charge-coupled Devices. Bellingham, Wash.: SPIE, 2001. Print. SPIE Monograph ; 83.

[12] Currie, Douglas G, David C Thompson, Steven E Buck, Rose P Des Georges, Cheng Ho, Dennis K Remelius, Bob Shirey, Thomas Gabriele, Victor L Gamiz, Laura J Ulibarri, Marc R Hallada, and Paul Szymanski. "Science Applications of the RULLI Camera: Photon Thrust, General Relativity and the Crab Nebula." 2005 AMOS Conference Proceedings (Advanced Maui Optical and Optical and Space Surveillance Technologies Conference) (2006): 2005 AMOS Conference Proceedings (Advanced Maui Optical and Optical and Space Surveillance Technologies Conference), 2006-01-01. Web.

[13] Roggemann, Michael C, Kris Hamada, Kim Luu, Venkata S Rao Gudimetla, Randy F Cortez, L William Bradford, David C Thompson, and Robert Shirey. "Three-Dimensional Imaging and Satellite Attitude Estimation Using Pulse Laser Illumination and a Remote Ultra-Low Light Imaging (RULLI) Sensor for Space Situational Awareness (SSA)." 2008 AMOS Conference Proceedings (Advanced Maui Optical and Optical and Space Surveillance Technologies Conference) (2008): 1. Web.

[14] Priedhorsky, William, and Jeffrey J Bloch. "Optical Detection of Rapidly Moving Objects in Space." Applied Optics (2004) 44.3 (2005): 423-33. Web.

[15] Bloch, Jeffrey J, and Richard Rast. "Space Surveillance One Photon at a Time." 2007 AMOS Conference Proceedings (Advanced Maui Optical and Optical and Space Surveillance Technologies Conference) (2007): 2007 AMOS Conference Proceedings (Advanced Maui Optical and Optical and Space Surveillance Technologies Conference), 2007-01-01. Web.

[16] Siegmund, Oswald, John Vallerga, Barry Welsh, Jason McPhate, Mike Rabin, and Jeffrey Bloch. "Advanced Photon Counting Imaging Detectors with 100ps Timing for Astronomical and Space Sensing Applications." *2005 AMOS Conference Proceedings (Advanced Maui Optical and Optical and Space Surveillance Technologies Conference)* (2006): 2005 AMOS Conference Proceedings (Advanced Maui Optical and Optical and Space Surveillance Technologies Conference), 2006-01-01. Web.
[17] McMahon-Crabtree, Peter N, and David G Monet. "Commercial-off-the-shelf Event-based Cameras for Space Surveillance Applications." Applied Optics (2004) 60.25 (2021): G144-153. Web.
[18] G. Cohen, S. Afshar, A. van Schaik, A. Wabnitz, T. Bessell, M. Rutten, and B. Morreale, "Event-based sensing for space situational awareness," Advanced Maui Optical and Space Surveillance Technologies Conference, Maui, Hawaii, USA, September 2017.
[19] B. Moomaw, "Camera technologies for low light imaging: overview and relative advantages," Methods Cell Biol. **114**, 243–283 (2013).
[20] M. Baker, "Faster frames, clearer pictures," Nat. Methods **8**(12), 1005–1009 (2011).
[21] Morimoto, K., J. Iwata, M. Shinohara, H. Sekine, A. Abdelghafar, H. Tsuchiya, Y. Kuroda, K. Tojima, W. Endo, Y. Maehashi, Y. Ota, T. Sasago, S. Maekawa, S. Hikosaka, T. Kanou, A. Kato, T. Tezuka, S. Yoshizaki, T. Ogawa, K. Uehira, A. Ehara, F. Inui, Y. Matsuno, K. Sakurai, and T. Ichikawa. "3.2 Megapixel 3D-Stacked Charge Focusing SPAD for Low-Light Imaging and Depth Sensing." 2021 IEEE International Electron Devices Meeting (IEDM) (2021): 20.2.1-0.2.4. Web.
[22] Morimoto, Kazuhiro, Andrei Ardelean, Ming-Lo Wu, Arin Can Ulku, Ivan Michel Antolovic, Claudio Bruschini, and Edoardo Charbon. "Megapixel time-gated SPAD image sensor for 2D and 3D imaging applications" Optica Vol. 7, Issue 4, pp. 346-354 (2020). Web.
[23] Zhang, Zhaoning, Yujie Wang, Rafael Piestun, and Zhen-li Huang. "Characterizing and Correcting Camera Noise in Back-illuminated SCMOS Cameras." *Optics Express* 29.5 (2021): 6668-690. Web.
[24] https://celestron-site-support-files.s3.amazonaws.com/support_files/RASA_White_Paper_2020_Web.pdf
[25] Canon Inc., 2021, 12, 15. "Canon develops SPAD sensor with world-highest 3.2-megapixel count, innovates with low-light imaging camera that realizes high color reproduction even in dark environments", Canon News Release. https://global.canon/en/news/2021/20211215.html.